Performance Comparison of Miniaturized Isolation Transformer Topologies

Yue Wu Charles R. Sullivan
Thayer School of Engineering at Dartmouth
Hanover, NH 03755 USA
Email: {Yue.Wu, Charles.R.Sullivan}@dartmouth.edu

Abstract—Seven different miniaturized low-power isolation transformer topologies are analyzed using FEA simulation. Performance optimizations of fixed-area transformers with different operation frequencies and heights, with and without magnetic cores, are performed. The comparison of optimization results reveals performance potential and trade-offs of the different topologies under different restrictions. More than 1 W of power transfer is possible at more than 85% efficiency in 1 mm^2 of footprint area for several different topologies.

I. Introduction

This paper is developing high performance miniaturized high frequency transformers with kV level isolation, delivering power in the range of 1 W. Such transformers can be applied to low power applications like IoT devices and can also be used in gate driving applications [1]–[5]. Seven different transformer topologies have been analyzed by FEA simulations. Optimizations were created using simulation-based performance results to compare the topologies. The results allow comparisons between the topologies at different operating frequencies and structural heights in the same packaging area to demonstrate the performance potential and unique characteristics of the topologies. The optimization tools developed in the process can also be used to design miniaturized high-performance high-isolation transformers. The seven transformer topologies (shown in Fig. 1) come from 3 different types of inductors, which are toroid, solenoid, and spiral inductors. Different inductor placements lead to the different transformer topologies. The end-to-end toroid is also a reasonable topology but was not analyzed. Based on results from other analyses, we do not expect it to perform well.

II. TRANSFORMER PERFORMANCE ANALYSIS

Because many of these air-core transformers have low coupling, their operation can be similar to that of a wireless power transfer system and we analyze them with the wireless power transfer framework presented in [6]. The maximum efficiency is:

$$\eta_{max} = \frac{\kappa^2 Q_1 Q_2}{(1 + \sqrt{1 + \kappa^2 Q_1 Q_2})^2} \tag{1}$$

where κ is the coupling coefficient, Q_1 , and Q_2 are the quality factors of the primary and secondary coils. But this

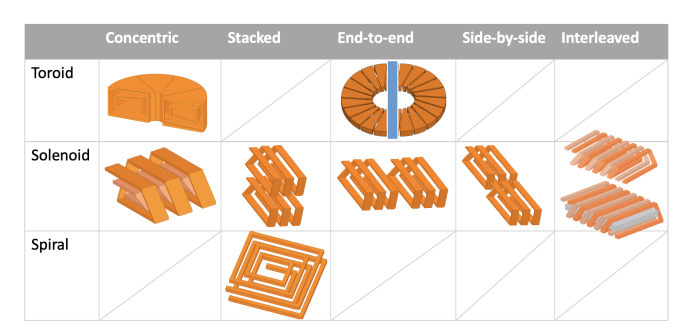


Fig. 1: Topologies based on 3 different inductor types categorized into 5 placement methods.

model simplifies the situation by ignoring the mutual resistance in a transformer. To test the accuracy of this model in different cases, a more comprehensive model developed based on the optimum operation analysis in [7] is used in comparison. The impedance matching techniques in [7] enable us to find the optimum efficiency of a transformer in a circuit simulator. Table. I shows the comparisons between the simplified model without mutual effect and the circuit simulator SIMPLIS on an optimized spiral sandwich (stacked spiral) design. When mutual resistance is low, the simplified model behaves identical to simulations. With additional tests on different designs with more mutual resistance, we conclude that when the mutual resistance is less than 20% of the coil resistance, ignoring it and using the simple model can estimate the transformer efficiency accurately enough while keeping the calculations simple.

TABLE I: Comparison of the efficiency results from simplified efficiency model and circuit simulator SIMPLIS.

Frequency	Impedance Matrix		Model	Simplis
30 MHz	$\begin{bmatrix} 0.32~\Omega, 21.8~\mathrm{nH} \\ 0.002~\Omega, 10.9~\mathrm{nH} \end{bmatrix}$	$\begin{bmatrix} 0.002 \; \Omega, 10.9 \; \mathrm{nH} \\ 0.32 \; \Omega, 21.8 \; \mathrm{nH} \end{bmatrix}$	72.9 %	72.9 %
119.4 MHz	$\begin{bmatrix} 0.66~\Omega, 21.2~\mathrm{nH} \\ 0.078~\Omega, 10.8~\mathrm{nH} \end{bmatrix}$	$\begin{bmatrix} 0.078 \; \Omega, 10.8 \; \mathrm{nH} \\ 0.66 \; \Omega, 21.2 \; \mathrm{nH} \end{bmatrix}$	85.0 %	85.1 %
$300~\mathrm{MHz}$	$\begin{bmatrix} 1.09 \ \Omega, 20.8 \ \mathrm{nH} \\ 0.188 \ \Omega, 10.7 \ \mathrm{nH} \end{bmatrix}$	$\begin{bmatrix} 0.188 \; \Omega, 10.7 \; \mathrm{nH} \\ 1.09 \; \Omega, 20.8 \; \mathrm{nH} \end{bmatrix}$	89.8%	89.9 %

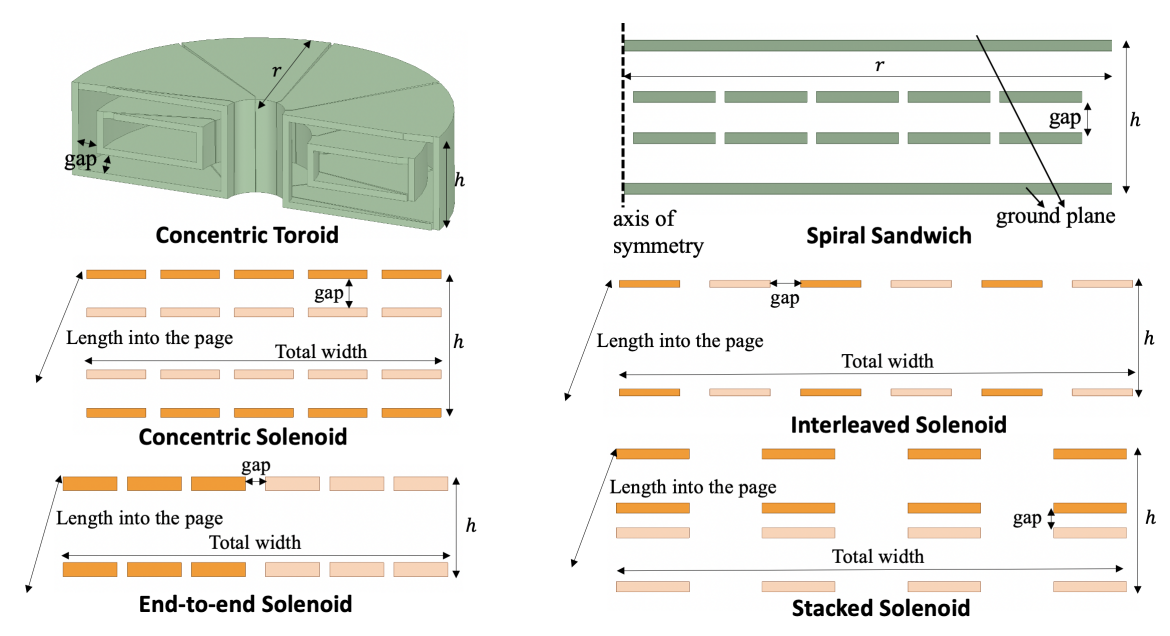


Fig. 2: Schematic for FEA simulation. For toroid and spiral, the area is defined by the radius. For solenoid, the area is the product of length into the page and total width.

III. TRANSFORMER DESIGN OPTIMIZATION

Ansys Maxwell is used to run FEA simulations to analyze the performance of the transformers. 3D FEA simulation is used for the concentric toroid transformer; axisymmetric 2D simulation is used for the spiral sandwich, and the rest of the topologies are analyzed with planar 2D simulations. Ansys Maxwell's built-in optimization tool is used to find the theoretical maximum performance of a topology under area, frequency, and height restrictions.

For a kV level isolation target and a polymer dielectric such as polyimide, we choose an isolation gap of 0.1 mm for all designs, based on a conservative estimate of $250V/\mu m$ practical dielectric withstand capability [4], [5], [8], [9]. All the conductor thicknesses are chosen to be 35 μm (1 oz copper). The important design parameters related to the optimization setups for all the topologies are shown in Fig. 2.

For all the solenoid topologies, the analysis assumes that the length into the page (as marked in Fig. 2) is much larger than the height, which turns out to be a category most of the optimization results belong to. If a design has its height larger than the length into the page, our analysis becomes an underestimate of the real performance. Since in normal integrated applications, the height is usually less than the length and width, we think the limitation in the analysis is a good trade-off to the speed of optimization. Our optimization results also show a similar level of per-area performance as the miniaturized transformers in [1]–[5]. It should be noted that the stacked and side-by-side solenoid share the same 2D FEA simulation setup. It is the relationship between length into the page and height defined the topology. The optimization results

all fall into the stacked category, which indicates that stacked solenoid is inherently a better performing topology than the side-by-side solenoid.

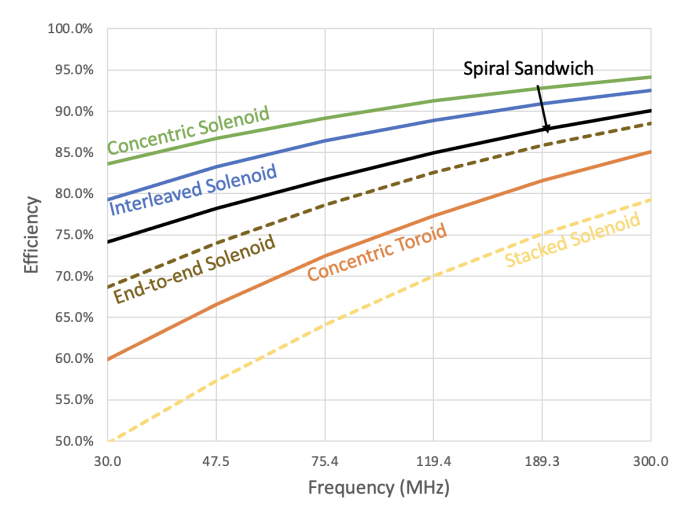
IV. AIR-CORE TOPOLOGY COMPARISON

Fig. 3a compares all the analyzed topologies over 30 to 300 MHz at a fixed height. The performance increases as frequency increases. End-to-end and stacked solenoids do not show good performance compared to others. Among the other topologies, concentric toroid has the advantage of low leakage inductance, the spiral is the easiest to fabricate due needing fewer metal layers, and the concentric and interleaved solenoids have the best performance. Using the figure can guide some design choices related to choosing the circuit operation frequency. If 85% efficiency is desired as well as low operating frequency, concentric solenoid will be a good choice. If high operating frequency is tolerable but fabrication cost is important, a spiral sandwich at 120 MHz may be a suitable option.

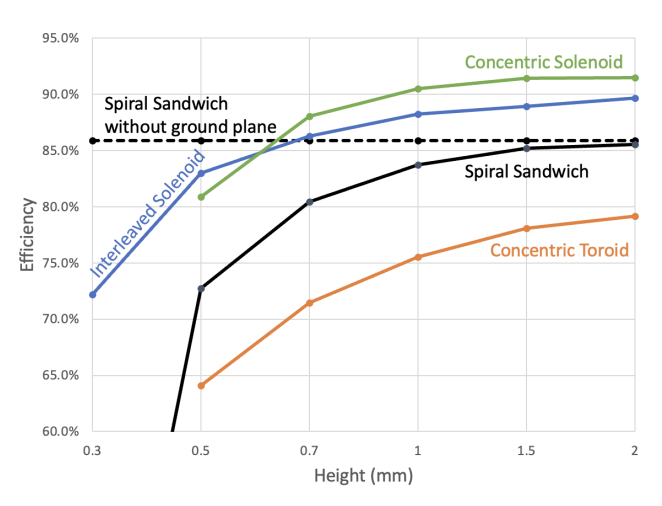
TABLE II: Leakage inductance and coupling factor for different topologies

Topology	Leakage Inductance		Magnetizing	Coupling
Topology	Primary	Secondary	Inductance	Factor
Concentric Solenoid	7.67 nH	3.19 nH	17.11 nH	0.750
Interleaved Solenoid	1.56 nH		4.81 nH	0.755
Spiral Sandwich	10.68 nH		12.28 nH	0.535
End-to-end Solenoid	13.78 nH		8.85 nH	0.391
Concentric Toroid	12.94 nH	0.15 nH	4.18 nH	0.485
Stacked Solenoid	14.00 nH		2.81 nH	0.167

The designs shown in this table are at 100 MHz with 1 mm height. The designs we analyzed have a 1:1 conversion ratio, thus some of them has identical primary and secondary windings.



(a) Comparison of different operating frequency at 1 mm height.



(b) Comparison of different structural height at 100 MHz.

Fig. 3: Topology comparison in 1 mm² area. The y-axis is the theoretical maximum efficiency of the topologies. The spiral sandwich has two ground planes to make them the same height as other topologies.

Table. II shows the leakage inductance and the coupling factor of the optimized designs at 100 MHz and 1 mm height for all the topologies shown in Fig. 3a. The concentric solenoid and the interleaved solenoid perform the best, while also having the best coupling and low leakage.

Fig. 3b shows a comparison between different topologies over 0.3 to 2 mm height at a fixed frequency for a selection of the best performing topologies. Due to multiple layers of metal and isolation needed in some topologies, not all topologies are viable at 0.3 mm height. If height is the primary concern, an interleaved solenoid is a very good option with above 70% efficiency. Choosing a higher operation frequency can also increase the performance. If the performance target is 85%, a concentric solenoid at 0.6 mm or a spiral sandwich at 1.5

mm are both valid options. This figure helps to demonstrate the trade-offs in height and efficiency between different topologies.

V. MAGNETIC MATERIAL

Among the best air-core topologies, the height of the topology has a large impact in performance. The usage of magnetic material can make it possible to have both low height and good performance. The interleaved solenoid is a promising candidate due to high performance and small height requirement.

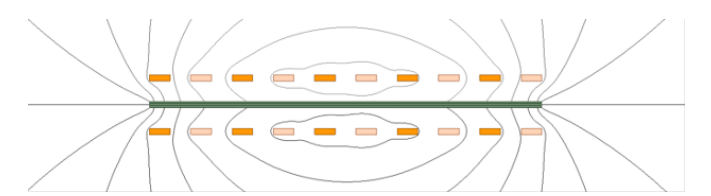


Fig. 4: Simulated flux line result with magnetic core.

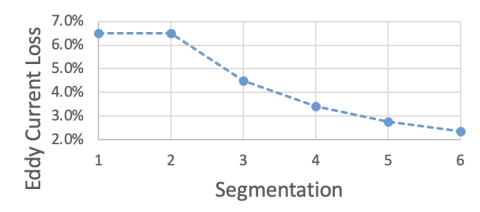
For the magnetic material, we choose Co-Zr-O as the core material. Co-Zr-O is one of the lowest loss material available with higher saturation flux density than ferrite. Nano-granular Co-Zr-O thin-film material can have a saturation flux density of 1 T, resistivity of 300 $\mu\Omega/cm$, and a relative permeability of 100 [10]. Models on its hysteresis effect and in-plane eddycurrent effect are developed in [10], [11]. The simulation result in Fig. 4 shows that there are flux lines perpendicular to the magnetic core, which causes out-of-plane eddy-current losses. Comparing it to the hysteresis and in-plane eddy-current effects, the simulation shows that the out-of-plane effect is significant. Thus, FEA simulation is essential for accurate analysis of the core loss. In analyzing the eddy-current effect in the magnetic core, we noticed that adding segmentation in either the width or the length into the page directions (as defined in Fig. 2) can reduce the magnetic loss. Because of the 2D FEA simulation setup for this analysis, we added segmentation as in the width direction as shown in Fig. 5a to improve the design's performance. Fig. 5b demonstrates the impact of segmentation to the overall core eddy-current loss. With six segments, the eddy-current loss can be reduced by 60% compared to designs without segmentation.

VI. MAGNETIC-CORE TOPOLOGY COMPARISON

Fig. 6a shows a comparison between different topologies over 30 to 300 MHz for a selection of the best performing topologies. Magnetic core and different heights are included. Unlike the air-core designs, the magnetic-core design has a best performing frequency. For this specific set of restrictions demonstrated by the brown curve in the figure, 60 MHz has the best performance. At 50 MHz, the magnetic-core design almost matches the performance of the best air-core design with 1/3 of the height. To achieve minimal height, the magnetic-core can be an option at up to 100 MHz.



(a) Segmentation demonstration.



(b) Segmentation vs core eddy-current loss.

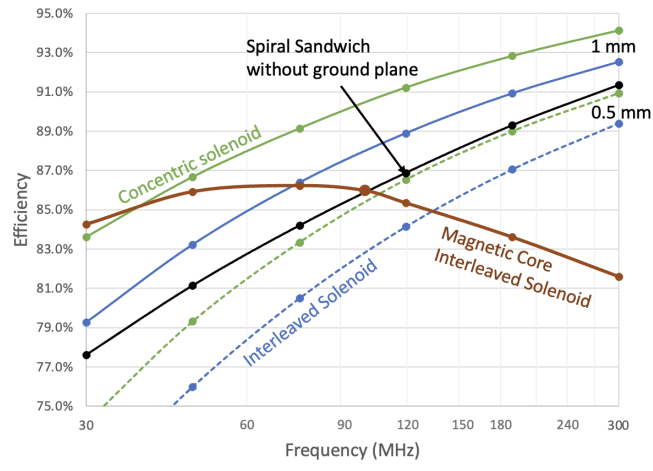
Fig. 5: Demonstration and performance impact of core segmentation.

Fig. 6b shows a similar performance comparison to Fig. 6a, but with magnetic core segmentation included, to demonstrate its potential at high frequencies. The usage of core segmentation increases the frequency for the best performance with a magnetic core. The 3-segmentation interleaved solenoid topology has identical performance as the air-core interleaved solenoid with only 1/3 the height at 100 MHz. If 6-segmentation is tolerable in fabrication, the magnetic core design can have 90% efficiency at 300 MHz.

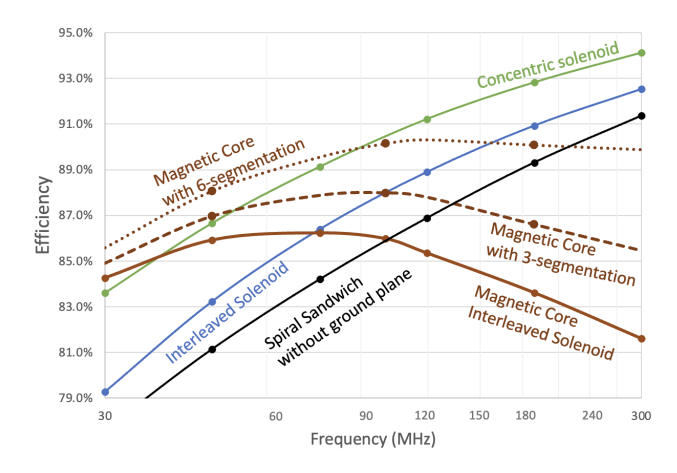
VII. CORE SEGMENTATION DESIGN

Demonstrated by the simulation results in previous sections, core segmentation is an effective approach for reducing the eddy-current loss in magnetic cores. Combining proper segmentation and lamination, the eddy-current loss in magnetic core can be minimized. The lamination is effective mostly on the in-plane eddy-effect [10], [11], while the segmentation is effective mostly on the out-of-plane eddy-effect. Due to the unevenness of the out-of-plane field, the induced eddy-current is also uneven in the width direction (as defined in Fig.2). From simulation result in Fig. 4, little out-of-plane field is present in the middle of the design, which also explains why having two segments evenly distributed is not improving the performance. As the out-of-plane flux is stronger to the edge than the middle, it is intuitive to have more segments on the edges than in the middle. Quantitative optimizations were performed to find out the best segmentation distribution.

Fig. 7 shows the optimization results of 5 and 7 segments of the core. Comparing each segment to the total width of the design, the 5-segment design has segment lengths of: 7%, 13%, 60%; the 7-segment design has segment lengths of: 3.7%, 6.8%, 11.6%, 55.6%. If regard the largest segment as two segments, the lengths of the 5-segments are: 7%, 13%, 30%; the lengths of the 7-segments are: 3.7%, 6.8%, 11.6%, 27.8%. Each design has a segment length that is approximately following a pattern of $\frac{2^i}{2^{n-1}-2}$ in comparison to the total width,



(a) Comparison with height difference, dashed lines are $0.5\ \mathrm{mm}$, solid lines are $1\ \mathrm{mm}$.



(b) Comparison with core segmentation.

Fig. 6: Topology comparison with magnetic corea and core segmentation design. All the designs analyzed are in 1 mm² area. The height of all magnetic-core designs is 0.29 mm. The y-axis is the theoretical maximum efficiency of the topologies. The spiral sandwich without ground plane can also be regard as two ground planes with infinite height.

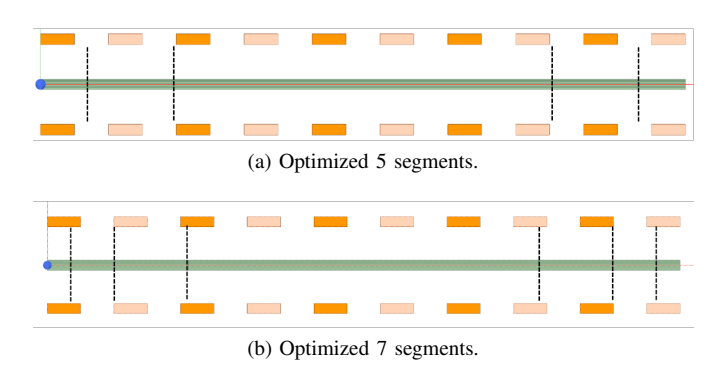


Fig. 7: Optimized segmentation designs.

where n is the number of segments and i goes from 0 to $\frac{n-1}{2}$. This pattern can be used to find a good core segmentation in magnetic designs like the interleaved solenoid transformer without computationally intensive optimization. Designs utilizing this core segmentation pattern have significant performance improvements compared to evenly distributed segments. Fig. 8 compares the optimized 5-segment design and an evenly distributed 6-segment design. The optimized 5-segment designs have about a 20% advantage in eddy-loss in the magnetic core compared to the evenly distributed 6-segment designs. Comparing the optimized 5-segment design with an ideal infinite-segment design, the performance is almost identical at low frequency. But at high frequencies where the eddyeffect becomes stronger, having more segments can still be beneficial.

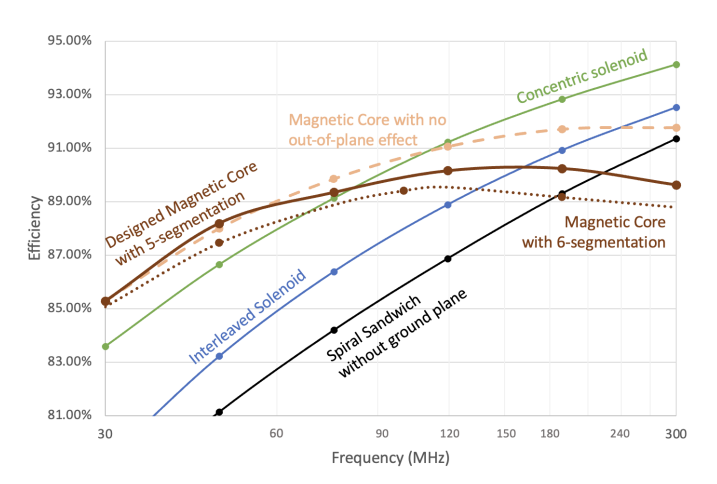


Fig. 8: Topology comparison with magnetic core. All the designs analyzed are in 1 mm² area. The height of all magnetic-core designs is 0.29 mm. The y-axis is the theoretical maximum efficiency of the topologies. The magnetic core with no out-of-plane effect is demonstrating the potential of infinite number of segments.

TABLE III: Leakage inductance and coupling factor comparison for air-core and magnetic-core designs

Topology	Leakage Inductance	Magnetizing Inductance	Coupling Factor
Air-core	1.56 nH	4.81 nH	0.755
Magnetic-core, no segmentation	1.51 nH	6.54 nH	0.817
Magnetic-core, 5 designed segment	1.46 nH	6.55 nH	0.818

The designs shown in this table are interleaved solenoid at 100 MHz. The air-core design is 1 mm in height, the magnetic-core designs are 0.29 mm.

Table. III shows the leakage inductance and the coupling factor of the interleaved solenoid transformer with air-core and magnetic-core. The addition of the core increases the coupling and magnetizing inductance, while reducing the leakage. It should be noted that the magnetic-core with 5 segments follows the segmentation method proposed in section VII. And all the segmentation analysis is based on an ideal case where there

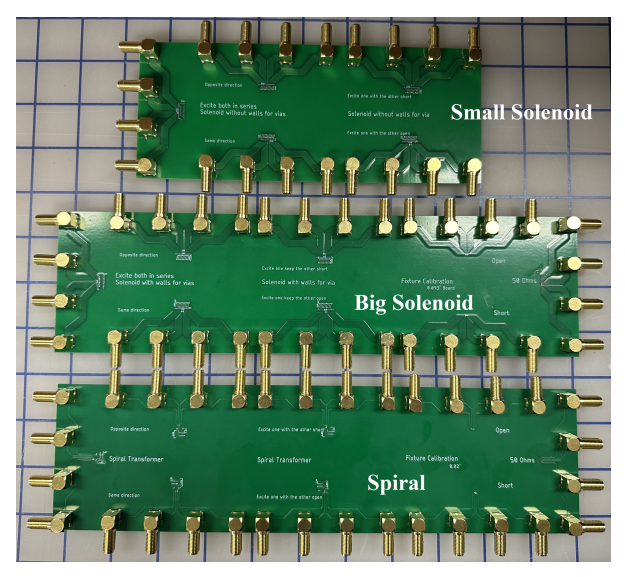


Fig. 9: Two air-core interleaved solenoid and a spiral fabricated on PCB. The solenoids are 2.55 mm in height, the spiral is 0.90 mm in height.

is no gap between core segments. With fabrication constraints, having more segments will mean less core material, which means more segments can lead to worse performance when little core material is left.

VIII. MEASUREMENT RESULTS

Fig. 9 illustrates three PCB transformers fabricated on a printed circuit board. For measurement purposes, five different connection methods of the transformer (demonstrated in Fig. 10) as well as calibration for the connection fixture are included on the boards. An Agilent 4294A impedance analyzer was used for the measurement. The designs chosen to be fabricated are the two best-performing topologies which only need two layers of metal structure, the interleaved solenoid and spiral. Due to limitations in fabrication and measurement, the fabricated design are based on the optimized designs at 64 MHz and all dimensions scaled up 4 times. Using analysis methods for scaling magnetic components proposed in [12], the inductance can be expressed as: $L = \frac{N^2 \mu_0 A_m}{l_m} \label{eq:loss}$

$$L = \frac{N^2 \mu_0 A_m}{l_m} \tag{2}$$

where N is the number of turns, μ_0 is vacuum permeability, A_m is the area of the flux path, and l_m is the length of the flux path. When all the dimensions are scaled up by by $4\times$, A_m will be scaled up by $16\times$, and l_m will be scaled up by 4×. Thus, the inductance of the scaled-up transformer winding will be increased by $4\times$. The ac resistance, on the other hand, can be expressed as:

$$R_{ac} = \frac{\rho N l_{turn}}{\delta w_w} \tag{3}$$

where ρ is the resistivity, l_{turn} is the length of winding per turn, δ is the skin depth, and w_w is the width of the winding.



(a) Measuring one winding with the other open.



(c) Measuring two winding in series in the same direction.



(e) Measuring one winding while exciting the other.



(b) Measuring one winding with the other short.



(d) Measuring two winding in series in the opposite direction.



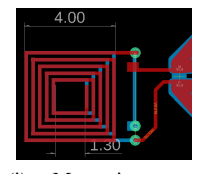
(f) Measuring one winding with the other open.



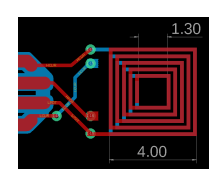
(g) Measuring one winding with the other short.



(h) Measuring two winding in series in the same direction.



(i) Measuring two winding in series in the opposite direction.



(j) Measuring one winding while exciting the other.

Fig. 10: A close-up look at the connection details of the small solenoid and spiral transformer on PCB. (a) to (e) are the small solenoid, (f) to (j) are the spiral. The setups for the big solenoid are similar to that shown here.

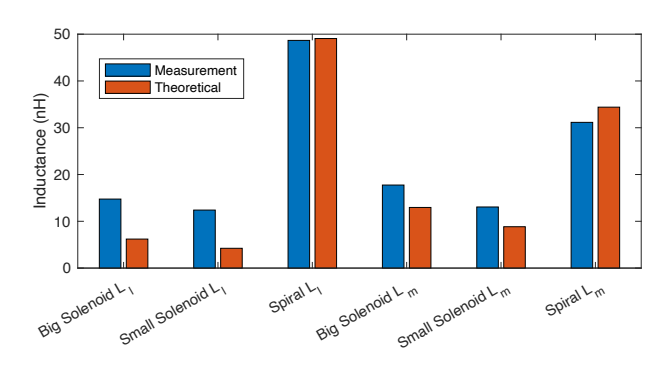
When all the dimensions are scaled up by $4\times$, l_{turn} and w_w will both be scaled up by $4\times$. As the transformer shape is unchanged in the scaling process, the coupling coefficient will be unchanged. To keep the performance of the scaled up transformer the same as before scaling, we find that when operating at 4 MHz, the factor of 1/16 in frequency will leave the quality factor $Q = \frac{\omega L}{R_{ac}}$ unchanged. As a result, the measurement of the PCB transformers at 4 MHz will directly reflect the performance of the optimized transformer operating at 64 MHz.

Table. IV shows the geometrical parameters and the measurement results of the fabricated PCB transformers. Fig. 11 shows a comparison of the measurement data and the theoretical analysis. The spiral transformer's analysis and measurement match very well. The analysis is based on a 2D axisymmetric FEA simulation of a round spiral. The results are converted for the square spiral using ways in [13]. The interleaved solenoid transformers have a more significant in-

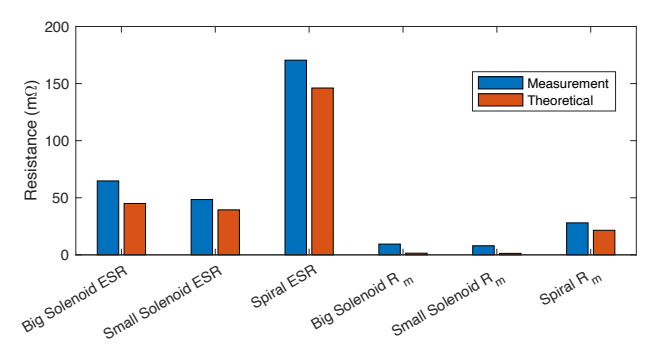
TABLE IV: PCB Transformer Measurement Results

Parameter	Large Solenoid	Small Solenoid	Spiral			
Number of Turns	5	5	5			
Length into the page (mm)	2.2	1.5				
Width (mm)	8.6	8.6	4			
Trace Width (mm)	0.35	0.35	0.15			
Trace Spacing (mm)	0.4	0.4	0.15			
Height (mm)	2.55	2.55	0.9			
Measurements						
L _{leakage} (nH)	14.75	12.40	48.67			
$L_{magnetizing}$ (nH)	17.75	13.06	31.15			
ESR (m Ω)	64.74	48.42	170.51			
$R_{mutual} (m\Omega)$	9.42	7.95	28.00			
Coupling Factor (%)	54.6	51.3	39.0			

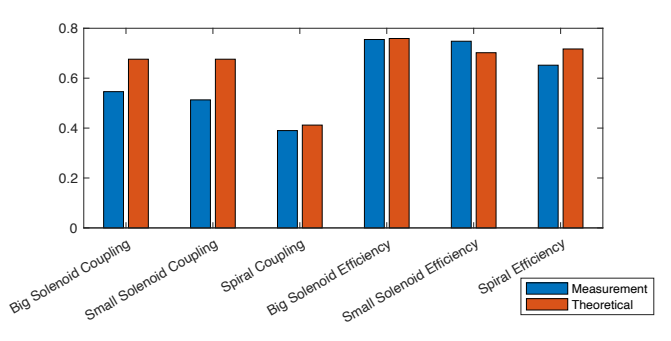
The geometrical parameters of the designs are marked in Fig. 2. Measurement results are at 4 MHz.



(a) Leakage inductance and magnetizing inductance comparison.



(b) ESR and mutual resistance comparison.



(c) Coupling factor and efficiency comparison.

Fig. 11: Measurement result vs theoretical data at 4 MHz.

ductance error, which is due to the transformers' length into the page being smaller than their height. Our analysis thus became an underestimate of the solenoid's real performance, which will not impair the conclusions we have on the comparisons between topologies. The mutual resistance has large percentage error, but the absolute error is less than $10 \text{ m}\Omega$, which is close to the resolution of our measurement setup. Seeing the other resistance measurements showing valid results, we think the resistance result is overall supporting our modeling method. Furthermore, all the efficiency comparison between theoretical and measurements are within a small margin of error. The measurement results demonstrate the validity of the topology comparisons based on the modeling method we used in this paper. Fig. 12 demonstrates the ESR and Q measurements for the three PCB transformers from 1 MHz to 10 MHz. The ESR of the spiral ramps up faster than the solenoids due to more eddy-current loss induced in the structure.

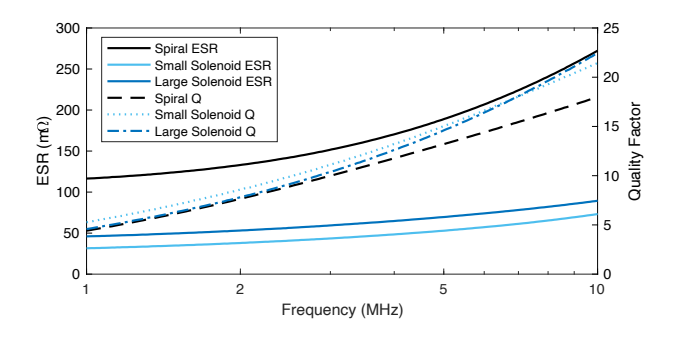


Fig. 12: ESR and Q measurements from 1 MHz to 10 MHz.

IX. CONCLUSION

This paper analyzed seven different air and magnetic-core transformer topologies. A tool was developed to find the best designs under certain area, height, and frequency restrictions. A selection of the optimized designs was fabricated and tested to verify our analysis. Among the air-core designs, the concentric and interleaved solenoid offer the best performance, followed by the spiral sandwich. The concentric toroid has acceptable performance with the advantage of low leakage flux. The Co-Zr-O magnetic-core interleaved solenoid with core segmentation can match good air-core designs at up to 100 MHz with much lower height.

ACKNOWLEDGMENT

This research was supported by the Power Management Integration Center, an NSF I/UCRC, under grant number 1822140.

REFERENCES

 D. Dinulovic, M. Shousha, and M. Haug, "Tiny Wafer Level Chip Scale Packaged Inductive Components for High Frequency Isolated/Non-Isolated DC-DC Converters," in 2021 IEEE Applied Power Electronics Conference and Exposition (APEC), Jun. 2021, pp. 1743–1746, iSSN: 2470-6647.

- [2] Y. Zhuo, S. Ma, T. Zhao, W. Qin, Y. Zhao, Y. Guo, H. Yan, and B. Chen, "A 52% Peak Efficiency gt; 1-W Isolated Power Transfer System Using Fully Integrated Transformer With Magnetic Core," *IEEE Journal of Solid-State Circuits*, vol. 54, no. 12, pp. 3326–3335, Dec. 2019, conference Name: IEEE Journal of Solid-State Circuits.
- [3] P. Lombardo, V. Fiore, E. Ragonese, and G. Palmisano, "16.7 A fully-integrated half-duplex data/power transfer system with up to 40Mb/s data rate, 23mW output power and on-chip 5kV galvanic isolation," in 2016 IEEE International Solid-State Circuits Conference (ISSCC), Jan. 2016, pp. 300–301, iSSN: 2376-8606.
- [4] N. Greco, A. Parisi, P. Lombardo, N. Spina, E. Ragonese, and G. Palmisano, "A Double-Isolated DC–DC Converter Based on Integrated \$LC\$ Resonant Barriers," *IEEE Transactions on Circuits and Systems I: Regular Papers*, vol. 65, no. 12, pp. 4423–4433, Dec. 2018, conference Name: IEEE Transactions on Circuits and Systems I: Regular Papers.
- [5] E. Ragonese, N. Spina, A. Castorina, P. Lombardo, N. Greco, A. Parisi, and G. Palmisano, "A Fully Integrated Galvanically Isolated DC-DC Converter With Data Communication," *IEEE Transactions on Circuits and Systems I: Regular Papers*, vol. 65, no. 4, pp. 1432–1441, Apr. 2018, conference Name: IEEE Transactions on Circuits and Systems I: Regular Papers.
- [6] Z. Zhang, H. Pang, A. Georgiadis, and C. Cecati, "Wireless Power Transfer—An Overview," *IEEE Transactions on Industrial Electronics*, vol. 66, no. 2, pp. 1044–1058, Feb. 2019, conference Name: IEEE Transactions on Industrial Electronics.
- [7] E. Waffenschmidt and T. Staring, "Limitation of inductive power transfer for consumer applications," in 2009 13th European Conference on Power Electronics and Applications, Sep. 2009, pp. 1–10.
- [8] E. Ragonese, N. Spina, A. Parisi, and G. Palmisano, "An Experimental Comparison of Galvanically Isolated DC-DC Converters: Isolation Technology and Integration Approach," *Electronics*, vol. 10, no. 10, p. 1186, Jan. 2021, number: 10 Publisher: Multidisciplinary Digital Publishing Institute. [Online]. Available: https://www.mdpi.com/2079-9292/10/10/1186
- [9] R. Tarzwell and K. Bahl, "High Voltage Printed Circuit Design & Manufacturing Notebook," p. 36.
- [10] D. Yao, "Microfabricated Thin-Film Inductors for High-Frequency DC-DC Power Conversion," Ph.D., Dartmouth College, United States – New Hampshire, 2011, iSBN: 9781267158635 Publication Title: ProQuest Dissertations and Theses. [Online]. Available: https://www.proquest.com/pqdtlocal1006600/docview/921493400/abstract/741DF158FB894C2APQ/2
- [11] D. V. Harburg, "Micro-fabricated racetrack inductors with thin-film magnetic cores for on-chip power conversion," Ph.D., Dartmouth College, United States New Hampshire, 2013, iSBN: 9781321135763 Publication Title: ProQuest Dissertations and Theses. [Online]. Available: https://www.proquest.com/pqdtlocal1006600/docview/1611959974/abstract/A6460CAC68F94FD6PQ/1
- [12] C. R. Sullivan, D. V. Harburg, J. Qiu, C. G. Levey, and D. Yao, "Integrating Magnetics for On-Chip Power: A Perspective," *IEEE Transactions on Power Electronics*, vol. 28, no. 9, pp. 4342–4353, Sep. 2013.
- [13] Y. Wu and C. R. Sullivan, "Optimizations and Comparisons of Air-Core Inductors Based on a Semi-Analytical Calculation Toolkit," in 2021 IEEE 22nd Workshop on Control and Modelling of Power Electronics (COMPEL), Nov. 2021, pp. 1–7, iSSN: 1093-5142.